Available online at www.sciencedirect.com
ScienceDirect
Composite Structures 77 (2007) 280–287
COMPOSITE STRUCTURES
www.elsevier.com/locate/compstruct

Analysis of sandwich TPS panel with functionally graded foam core by Galerkin method

H. Zhu, B.V. Sankar *

Department of Mechanical and Aerospace Engineering, University of Florida, P.O. Box 116250, Gainesville, FL 32611-6250, USA

Available online 2 September 2005

Abstract

The method of Fourier analysis is combined with the Galerkin method for solving the two-dimensional elasticity equations for a sandwich thermal protection system (TPS) insulation panel with foam core subjected to transverse loads. The variation of the Young's modulus through the thickness is given by a polynomial in the thickness coordinate and the Poisson's ratio is assumed to be constant. The Fourier series method is used to reduce the partial differential equations to a pair of ordinary differential equations, which are solved by using the Galerkin method. The method will be useful in analyzing functionally graded TPS structures with arbitrary variation of thermomechanical properties in the thickness direction. The analysis was also performed using sandwich plate theory. Significant differences were found in the results suggesting that the sandwich theory may not be suitable for the analysis of thick sandwich TPS panel.

Keywords: Thermal protection system; Sandwich panel; Foam core; Functionally graded materials; Galerkin method

1. Introduction

Thermal protection systems (TPS) on reusable launch vehicles (RLV) have to be designed such that the maximum temperature and stresses of the RLV tank structure is kept below a specified safe limit. A significant component of the total vehicle weight in addition to structural weight of the tanks is the weight of the thermal protection system. Sandwich structures can offer high stiffness with relatively much weight saving compared to widely used laminated structures. A recent study of TPS modeling and performance issues performed by Blosser et al. [1,2] has shown that currently existing Saffil foam-filled TPS tile weighs 5.85–19.3 kg/m^2 (1.2–3.96 lb/ft^2), while the structural weight ranges from 4.64 to 8.54 kg/m^2 (0.95–1.75 lb/ft^2). The enclosed volume of the TPS tile is filled with the Saffil (fibrous foam type) insulation. Since the Saffil insulation is flexible and cannot be attached directly, it needs encapsulation in a foil and the secondary TPS support structure. Metallic foams, which have low density, relatively low conductivity and some load-bearing ability, seem to be a promising candidate for insulation material besides Saffil insulation, if their relative density profiles are designed appropriately.

Functionally graded foams can improve the performance of the insulation. For steady state heat flow, Venkataraman et al. [3] optimized the solidity profile of the foam in order to minimize the transmitted heat for a given mass or minimize the thickness for a specified transmitted heat. It should be noted that solidity or volume fraction of foam is defined as the ratio between the volume of the solid material and the volume of foam. In a second paper Zhu et al. [4] minimized the TPS mass for specified heat transfer. Later a transient problem was solved in which the maximum structural temperature of a two layer insulation was minimized by varying

* Corresponding author. Tel.: +1 352 392 6749; fax: +1 352 392 7303.
E-mail address: sankar@ufl.edu (B.V. Sankar).

0263-8223/$ - see front matter © 2005 Elsevier Ltd. All rights reserved.
doi:10.1016/j.compstruct.2005.07.005

the solidity profile for a given total thickness and mass [5]. The two layers were assumed homogeneous with solidity being constant in each layer. It is shown that the cooler inner layer of optimal design has high solidity, while the hotter outer layer has low solidity. This is in contrast to the steady-sate optimum, where the solidity profile is the reverse.

The objective of this paper is to develop a thermal-structural analysis of a sandwich TPS panel subjected to transient heat conduction during reentry. The material properties such as Young's modulus, yield strength, thermal conductivity and coefficient of thermal expansion are assumed to be temperature dependent. Hence approximate methods such as finite difference method for heat conduction and Galerkin method for structural analysis have to be used. The sandwich panel is divided into four elements (two face sheets and two layers of core with different solidities). An elasticity solution is derived for each layer based on the procedures developed by Sankar et al. [6,7]. The solution for strains and stresses in the entire sandwich panel is obtained by enforcing the compatibility of tractions and displacements at the interfaces between each element. The Fourier series method is used to reduce the partial differential equations to a pair of ordinary differential equations, which are solved by using the Galerkin method. For the purpose of comparison, the panel is also analyzed by one-dimensional plate theory.

2. Analysis

In this section we identify the necessary information and modeling details required to perform structural analysis of the sandwich TPS panel. The heat transfer in the TPS panel is assumed to be one-dimensional. The finite width effects of the TPS insulation and the heat shorts resulting from the support structure around the perimeter of the TPS tile are ignored. The structural mass on the inside will correspond to the mass of the stiffened panel shell used for the RLV tank construction. The insulation itself is made of open cell titanium foam material.

The heat transfer in foams proceeds by three modes: conduction through the solid materials, conduction in the gas filling this foam and radiation inside the foam. The model used to calculate the heat transfer coefficient in the foam is discussed in Venkataraman et al. [3]. To minimize radiation it requires higher solidity foams (smaller foam pore sizes) while to minimize conduction it needs low solidity foams (large foam pore sizes). Since there is a temperature gradient through the insulation, an optimum insulation requires different solidities in different regions. Optimum density profiles of metallic foam insulations that minimize heat transmitted to the inside under transient steady-state heat transfer conditions are presented in Venkataraman et al. [3].

Fig. 1 shows a schematic of the cross-section of the simplified sandwich TPS panel. The length of the panel is 0.4572 m (18 in.). The top facesheet is made of homogeneous titanium plate with thickness 0.5 mm. The foam core is divided into two layers with total thickness 90 mm (3.54 in.). The solidity in each layer of foam core can vary continuously. The foam is idealized as having rectangular cells of uniform size. The variation in solidity is achieved by tailoring the cell size while keeping the strut diameter fixed at 0.05 mm (0.002 in.). The structural mass on the inside will correspond to the mass of the stiffened panel shell used for the RLV tank construction which is made of aluminum with thickness 2.2 mm (about 0.0866 in.). The areal density of structure is 6.1 kg/m^2 (1.25 lb/ft^2). The temperature dependent material properties of titanium and aluminum are the same as the material properties used in Ref. [8].

3. Structural analysis of the TPS panel

The TPS panel is assumed to be simply supported and in a state of plane strain normal to the z–x plane (one-dimensional plate). The governing equations are formulated for each layer. The solutions of strains and stresses of entire sandwich are obtained by enforcing the compatibility displacements and continuity of tractions at the interfaces between each layer, which is analogous to assembling element stiffness matrices in FEM

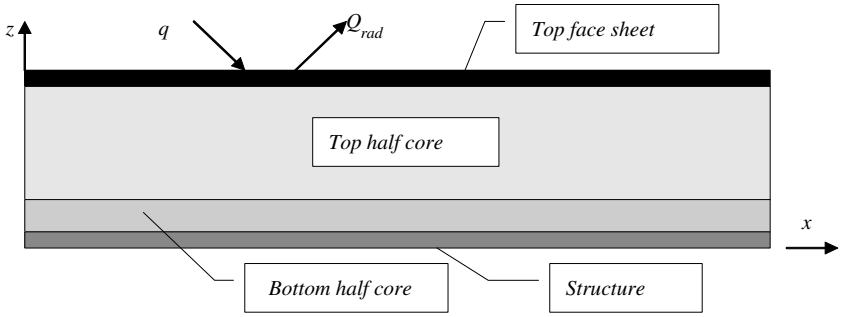

Fig. 1. Schematic of the cross-section of the sandwich TPS panel on a reusable launch vehicle structure.

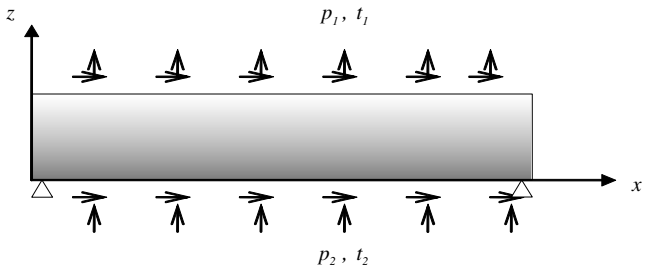

Fig. 2. Functionally graded beam subjected to symmetric loading.

analysis. We will derive the elasticity solution for a typical layer first.

3.1. Analysis of a single layer

Consider a functionally graded one-dimensional plate of height h and length L as shown in Fig. 2. The boundary conditions at the two edges of the plate, $x = 0$ and L, are similar to that of a simply supported plate. We assume that the functionally graded material is isotropic at every point and the Poisson's ratio v is a constant through the thickness. The variation of Young's modulus E in the thickness direction is given by a polynomial in z as

$$E(z) = E_0\left(a_1 + a_2\left(\frac{z}{h}\right) + a_3\left(\frac{z}{h}\right)^2 + a_4\left(\frac{z}{h}\right)^3\right) \tag{1}$$

There are normal and shear tractions applied on both top and bottom surfaces. The tractions are assumed to be symmetric about the centerline ($x = L/2$):

$$\begin{aligned} p_1 &= P_1 \sin \xi x \\ t_1 &= T_1 \cos \xi x \\ p_2 &= P_2 \sin \xi x \\ t_2 &= T_2 \cos \xi x \\ \xi &= \frac{n\pi}{L} \quad n = 1, 3, 5, \ldots \end{aligned} \tag{2}$$

The temperature distribution $\theta(x,z)$ at bottom surface is also assumed symmetric about the centerline ($x = L/2$). The temperature variation in the thickness direction follows same pattern for each x, which can be expressed in polynomial as

$$\begin{aligned} \theta(x,z) &= \left[\sum_{n=1}^{\infty} T_n \sin \xi x\right] \cdot \left[\sum_{\lambda=1}^{4} d_\lambda z^{\lambda-1}\right] \\ \xi &= \frac{n\pi}{L} \quad n = 1, 3, 5, \ldots \quad \lambda = 1, 2, 3, 4 \end{aligned} \tag{3}$$

We will solve the problem for one value of ξ. Let

$$\theta_{n\lambda}(x,z) = \sum_{\lambda=1}^{4} d_\lambda T_n z^{\lambda-1} \sin \xi x \tag{4}$$

Assume the displacements are in the form of

$$\begin{aligned} u(x,z) &= U(z) \cos \xi x \\ w(x,z) &= W(z) \sin \xi x \end{aligned} \tag{5}$$

The strains are derived as

$$\begin{aligned} \varepsilon_{xx} &= -U\xi \sin \xi x \\ \varepsilon_{zz} &= W' \sin \xi x \\ \gamma_{zz} &= (U' + W\xi) \cos \xi x \end{aligned} \tag{6}$$

Assuming that the principal material directions coincide with the x and z axes, the constitutive equations are:

$$\begin{Bmatrix} \sigma_{xx} \\ \sigma_{zz} \\ \tau_{xz} \end{Bmatrix} = \begin{bmatrix} c_{11} & c_{13} & 0 \\ c_{13} & c_{33} & 0 \\ 0 & 0 & c_{55} \end{bmatrix} \left\{ \begin{bmatrix} \varepsilon_{xx} \\ \varepsilon_{zz} \\ \gamma_{xz} \end{bmatrix} - \theta(x,z) \begin{bmatrix} \alpha_x(z) \\ \alpha_z(z) \\ 0 \end{bmatrix} \right\} \tag{7}$$

where $[C]$ can be expressed as

$$C^{-1} = \begin{pmatrix} \frac{1}{E_{11}} & \frac{-v_{13}}{E_{11}} & 0 \\ \frac{-v_{13}}{E_{11}} & \frac{1}{E_{33}} & 0 \\ 0 & 0 & \frac{1}{G_{13}} \end{pmatrix} \tag{8}$$

Eq. (6) can be rewritten as

$$\begin{Bmatrix} \sigma_{xx} \\ \sigma_{zz} \\ \tau_{xz} \end{Bmatrix} = \begin{bmatrix} c_{11} & c_{13} & 0 \\ c_{13} & c_{33} & 0 \\ 0 & 0 & c_{55} \end{bmatrix} \begin{bmatrix} \varepsilon_{xx} \\ \varepsilon_{zz} \\ \gamma_{xz} \end{bmatrix} - \begin{bmatrix} \beta_x(z) \\ \beta_z(z) \\ 0 \end{bmatrix} \cdot \sum_{\lambda=1}^{4} d_\lambda T_n z^{\lambda-1} \sin \xi x \tag{9}$$

where the β's can be expressed as

$$\begin{Bmatrix} \beta_x \\ \beta_z \\ 0 \end{Bmatrix} = \begin{bmatrix} c_{11} & c_{13} & 0 \\ c_{13} & c_{33} & 0 \\ 0 & 0 & c_{55} \end{bmatrix} \begin{bmatrix} \alpha_x(z) \\ \alpha_z(z) \\ 0 \end{bmatrix} \tag{10}$$

Substituting Eq. (6) into Eq. (9), we have,

$$\begin{aligned} \sigma_{xx} &= S_x(z) \sin \xi x \\ \sigma_{zz} &= S_z(z) \sin \xi x \\ \tau_{xz} &= T_z(z) \cos \xi x \end{aligned} \tag{11}$$

where

$$\begin{aligned} S_x &= (-c_{11} U\xi + c_{13} W' - d_\lambda T_n z^{\lambda-1} \beta_x(z)) \\ S_z &= (-c_{13} U\xi + c_{33} W' - d_\lambda T_n z^{\lambda-1} \beta_z(z)) \\ T_z &= c_{55}(U' + W\xi) \end{aligned} \tag{12}$$

The governing equilibrium equations are (body forces are neglected):

$$\begin{aligned} \frac{\partial \sigma_{xx}}{\partial x} + \frac{\partial \tau_{xz}}{\partial z} &= 0 \\ \frac{\partial \tau_{xz}}{\partial x} + \frac{\partial \sigma_{zz}}{\partial z} &= 0 \end{aligned} \tag{13}$$

Substituting Eq. (11) into Eq. (13), we obtain,

$$\begin{aligned} &\xi S_x(z) + T_z'(z) = 0 \\ &S_z'(z) - \xi T_z(z) = 0 \end{aligned} \tag{14}$$

Eq. (14) is solved by Galerkin method by assuming four basis functions:

$$\begin{aligned} &U(z) = c_j \phi_j(z) \\ &W(z) = b_j \phi_j(z) \quad j = 1,2,3,4 \end{aligned} \tag{15}$$

where

$$\phi_1(z) = 1; \quad \phi_2(z) = z; \quad \phi_3(z) = z^2; \quad \phi_4(z) = z^3 \tag{16}$$

Substituting the approximate solution in the governing differential equations, we obtain the residuals. The residuals are minimized by equating their weighted averages to zero:

$$\begin{aligned} &\int_0^h (\xi S_x + T_z')\phi_i(z)\,\mathrm{d}z = 0, \quad i = 1,2,3,4 \\ &\int_0^h (S_z' + T_z\xi)\phi_i(z)\,\mathrm{d}z = 0, \quad i = 1,2,3,4 \end{aligned} \tag{17}$$

Using integration by parts we can rewrite Eq. (17) as

$$\begin{aligned} &\int_0^h \phi_i \xi S_x\,\mathrm{d}z + T_z(h)\phi_i(h) - T_z(0)\phi_i(0) \\ &\quad - \int_0^h T_z \phi_i'\,\mathrm{d}z = 0, \quad i = 1,2,3,4 \\ &\int_0^h S_z \phi_i'\,\mathrm{d}z + \int_0^h T_z \xi \phi_i\,\mathrm{d}z - (S_z(h)\phi_i(h) \\ &\quad - S_z(0)\phi_i(0)) = 0, \quad i = 1,2,3,4 \end{aligned} \tag{18}$$

Substituting for $S_x(z)$, $S_z(z)$ and $T_z(z)$ from Eq. (12) into Eq. (18) and using the approximate solution for $U(z)$ and $W(z)$ in Eq. (15) we obtain:

$$\begin{pmatrix} K_{ij}^{(1)} & K_{ij}^{(2)} \\ K_{ij}^{(3)} & K_{ij}^{(4)} \end{pmatrix} \begin{pmatrix} b \\ c \end{pmatrix} = \begin{pmatrix} f_i^{(1)} \\ f_i^{(2)} \end{pmatrix} \tag{19}$$

where

$$\begin{aligned} K_{ij}^{(1)} &= \xi \int_0^h c_{13}\phi_i\phi_j'\,\mathrm{d}z - \xi \int_0^h c_{55}\phi_i'\phi_j\,\mathrm{d}z \\ K_{ij}^{(2)} &= -\int_0^h c_{55}\phi_i'\phi_j'\,\mathrm{d}z - \xi^2 \int_0^h c_{11}\phi_i\phi_j\,\mathrm{d}z \\ K_{ij}^{(3)} &= -\xi^2 \int_0^h c_{55}\phi_i\phi_j\,\mathrm{d}z - \int_0^h c_{33}\phi_i'\phi_j'\,\mathrm{d}z \\ K_{ij}^{(4)} &= \xi \int_0^h c_{13}\phi_i'\phi_j\,\mathrm{d}z - \xi \int_0^h c_{55}\phi_i\phi_j'\,\mathrm{d}z \\ f_i^{(1)} &= \phi_i(0)T_z(0) - \phi_i(h)T_z(h) \\ &\quad + \sum_{\lambda=1}^{4} \xi d_\lambda T_n \int_0^h z^{\lambda-1}\beta_x(z)\phi_i\,\mathrm{d}z \\ f_i^{(2)} &= \phi_i(0)S_z(0) - \phi_i(h)S_z(h) \\ &\quad - \sum_{\lambda=1}^{4} d_\lambda T_n \int_0^h z^{\lambda-1}\beta_x(z)\phi_i'\,\mathrm{d}z \end{aligned} \tag{20}$$

$$D = \begin{pmatrix} b \\ c \end{pmatrix}^{\mathrm{T}} = (\,b_1 \quad b_2 \quad b_3 \quad b_4 \quad c_1 \quad c_2 \quad c_3 \quad c_4\,) \tag{21}$$

The boundary conditions at both top and bottom surface are shown as following:

At top surface

$$\begin{aligned} &t_1 = T_1 \cos \xi x \\ &p_1 = P_1 \sin \xi x \end{aligned} \tag{22}$$

Hence we have

$$\begin{aligned} &S_z(h) = P_1 \\ &T_z(h) = T_1 \end{aligned} \tag{23}$$

At bottom surface

$$\begin{aligned} &t_2 = T_2 \cos \xi x \\ &p_2 = P_2 \sin \xi x \end{aligned} \tag{24}$$

which yields

$$\begin{aligned} &S_z(0) = -P_2 \\ &T_z(0) = -T_2 \end{aligned} \tag{25}$$

Substituting Eqs. (23) and (25) into Eq. (20), $[f]$ in Eq. (20) can be rewritten as

$$\begin{bmatrix} f_1^{(1)} \\ f_2^{(1)} \\ f_3^{(1)} \\ f_4^{(1)} \\ f_1^{(2)} \\ f_2^{(2)} \\ f_3^{(2)} \\ f_4^{(2)} \end{bmatrix} = - \begin{bmatrix} \phi_1(h) & 0 & \phi_1(0) & 0 \\ \phi_2(h) & 0 & \phi_2(0) & 0 \\ \phi_3(h) & 0 & \phi_3(0) & 0 \\ \phi_4(h) & 0 & \phi_4(0) & 0 \\ 0 & \phi_1(h) & 0 & \phi_1(0) \\ 0 & \phi_2(h) & 0 & \phi_2(0) \\ 0 & \phi_3(h) & 0 & \phi_3(0) \\ 0 & \phi_4(h) & 0 & \phi_4(0) \end{bmatrix} \cdot \begin{bmatrix} T_1 \\ P_1 \\ T_2 \\ P_2 \end{bmatrix} + d_\lambda T_n \begin{bmatrix} \xi \int_0^h z^{\lambda-1}\beta_x(z)\phi_1\,\mathrm{d}z \\ \xi \int_0^h z^{\lambda-1}\beta_x(z)\phi_2\,\mathrm{d}z \\ \xi \int_0^h z^{\lambda-1}\beta_x(z)\phi_3\,\mathrm{d}z \\ \xi \int_0^h z^{\lambda-1}\beta_x(z)\phi_4\,\mathrm{d}z \\ -\int_0^h z^{\lambda-1}\beta_z(z)\phi_1'\,\mathrm{d}z \\ -\int_0^h z^{\lambda-1}\beta_z(z)\phi_2'\,\mathrm{d}z \\ -\int_0^h z^{\lambda-1}\beta_z(z)\phi_3'\,\mathrm{d}z \\ -\int_0^h z^{\lambda-1}\beta_z(z)\phi_4'\,\mathrm{d}z \end{bmatrix} \tag{26}$$

or

$$f = \Phi P + M \tag{27}$$

Eq. (15) can be expanded as

$$\begin{bmatrix} U_1 \\ W_1 \\ U_2 \\ W_2 \end{bmatrix} = \begin{bmatrix} 0 & 0 & 0 & 0 & 1 & h & h^2 & h^3 \\ 1 & h & h^2 & h^3 & 0 & 0 & 0 & 0 \\ 0 & 0 & 0 & 0 & 1 & 0 & 0 & 0 \\ 1 & 0 & 0 & 0 & 0 & 0 & 0 & 0 \end{bmatrix} \begin{bmatrix} b_1 \\ b_2 \\ b_3 \\ b_4 \\ c_1 \\ c_2 \\ c_3 \\ c_4 \end{bmatrix} \tag{28}$$

or

$$U = HD \tag{29}$$

Now we have three equatipns (19), (27) and (29). From these three equations, we obtain,

$$U = HK^{-1}[\Phi P + M] = K^* P + M^* \tag{30}$$

or

$$P = SU - R \tag{31}$$

where

$$\begin{aligned} S &= [K^*]^{-1} \\ R &= [K^*]^{-1} M^* \end{aligned} \tag{32}$$

3.2. Analysis of the whole panel

Assume displacements are in the form:

$$\begin{aligned} p_i &= P_i \sin \xi x \\ t_i &= T_i \cos \xi x \quad i = 1, 2, 3, 4, 5 \\ \xi &= \frac{n\pi}{L} \quad n = 1, 3, 5, \ldots \end{aligned} \tag{33}$$

For given temperature distribution in each layer:

$$P^{(i)} = S^{(i)} U^{(i)} - R^{(i)} \tag{34}$$

In order to satisfy equilibrium, the contribution of the different tractions at each interface should sum to zero. Enforcing the balance of force and displacement at the interface, we got global stiff matrix S_G:

$$S_G \begin{bmatrix} U_1 \\ W_1 \\ U_2 \\ W_2 \\ U_3 \\ W_3 \\ U_4 \\ W_4 \\ U_5 \\ W_5 \end{bmatrix} - \begin{bmatrix} R_1^{(1)} \\ R_2^{(1)} \\ R_3^{(1)} \\ R_4^{(1)} \\ 0 \\ 0 \\ 0 \\ 0 \\ 0 \\ 0 \end{bmatrix} - \begin{bmatrix} 0 \\ 0 \\ R_1^{(2)} \\ R_2^{(2)} \\ R_3^{(2)} \\ R_4^{(2)} \\ 0 \\ 0 \\ 0 \\ 0 \end{bmatrix} - \begin{bmatrix} 0 \\ 0 \\ 0 \\ 0 \\ R_1^{(3)} \\ R_2^{(3)} \\ R_3^{(3)} \\ R_4^{(3)} \\ 0 \\ 0 \end{bmatrix} - \begin{bmatrix} 0 \\ 0 \\ 0 \\ 0 \\ 0 \\ 0 \\ R_1^{(4)} \\ R_2^{(4)} \\ R_3^{(4)} \\ R_4^{(4)} \end{bmatrix} = \begin{bmatrix} T_1 \\ P_1 \\ 0 \\ 0 \\ 0 \\ 0 \\ 0 \\ 0 \\ T_5 \\ P_5 \end{bmatrix} \tag{35}$$

Solving the above Eq. (35), we can obtain the displacement field for each layer. The displacement field and the constitutive equations can be used to obtain the stress filed in each layer.

Sankar and Tzeng [7] derived the one-dimensional plate theory following the Euler–Bernoulli beam assumption. He also neglected the normal stresses in thickness direction σ_{zz}. We followed a similar procedure to derive a sandwich beam theory for the composite sandwich panel and compare this solution with the approximate elasticity solution by Galerkin method.

4. Numerical results

The analysis procedures described in the preceding section was used to calculate the stresses in a TPS panel during the reentry of the vehicle. Based on our previous work of minimizing the maximum temperature of a structure [4], we found that the cooler inner layer of the optimal two-layer design has high solidity, while the hotter outer layer has low solidity. Hence we vary the solidity of foam linearly from 0.11 at bottom to 0.01 at top surface, which is called as linear design. It should be noted that the elastic constants of metal foams depend on the foam solidity. Choi and Sankar [9] derived an expression for the Young's modulus of a cellular solid as

$$E_f = \frac{1}{3}\rho E_s \tag{36}$$

where ρ is the solidity and the subscripts f and s, respectively, refer to the homogenized foam and the strut material. In our study, the heat flux and pressure on the vehicle during reentry are obtained from Blosser et al. [1,2]. The heat flux varies significantly over the surface. For our study we choose a location on the windward surface referred to as station 1199 (STA 1199) as a representative point for the point design [8].

The stress variations with respect to time at various locations of the sandwich TPS panel with length 0.4572 m (18 in.) are presented in Figs. 3–6. It can be noted that both sandwich and Galerkin solutions agree well with each other, which means sandwich theory can provide relatively accurate results for slender beam ($L/H = 4.9$). We also compared the two solutions for beam with length $L = 225$ mm (9 in.) ($L/H = 2.46$). The results are shown in Figs. 7–10. The maximum difference between theses two solution for stresses in the structure is 18%, which suggests that the sandwich theory may not be suitable for the analysis of thick sandwich TPS panel.

We also investigate the performance of functionally graded foam insulation for transient heat transfer condition by comparing it with the uniform solidity foam

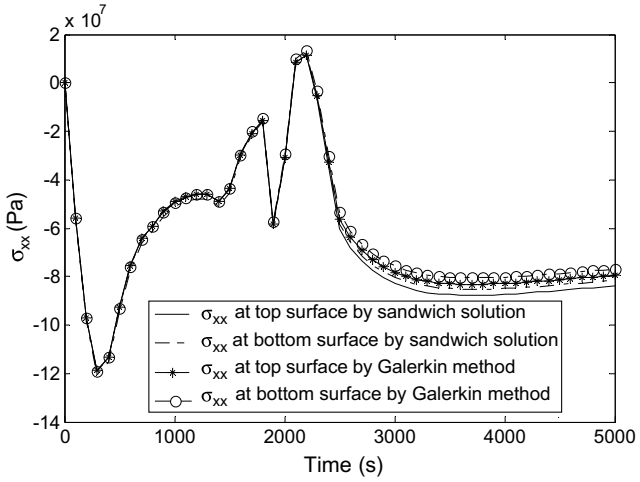

Fig. 3. History of normal stress (σ_{xx}) in top facesheet of linear design ($L = 18$ in.).

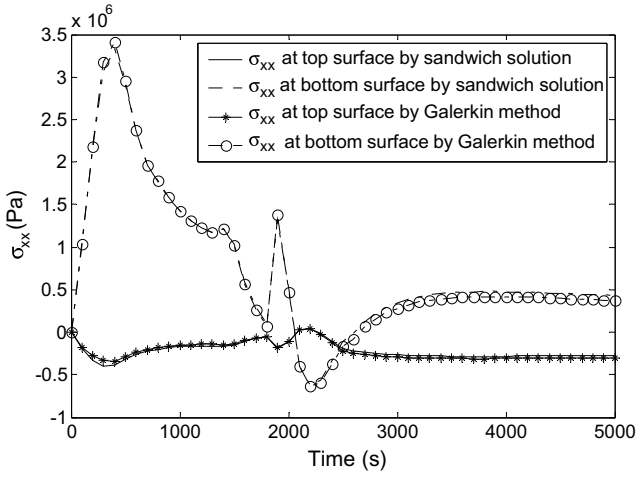

Fig. 4. History of normal stress (σ_{xx}) in top half core of linear design ($L = 18$ in.).

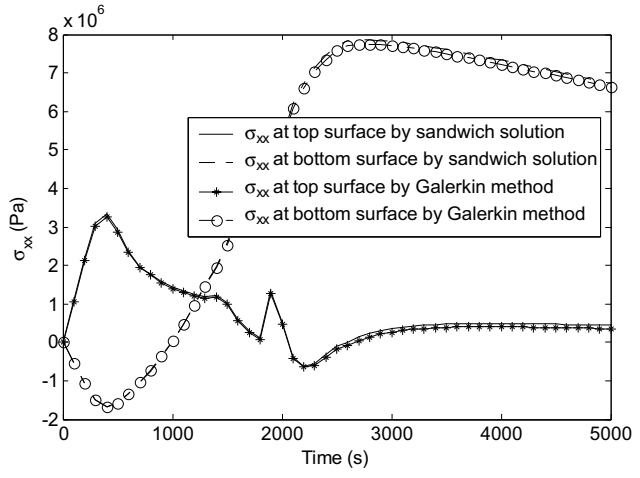

Fig. 5. History of normal stress (σ_{xx}) in bottom half core of linear design ($L = 18$ in.).

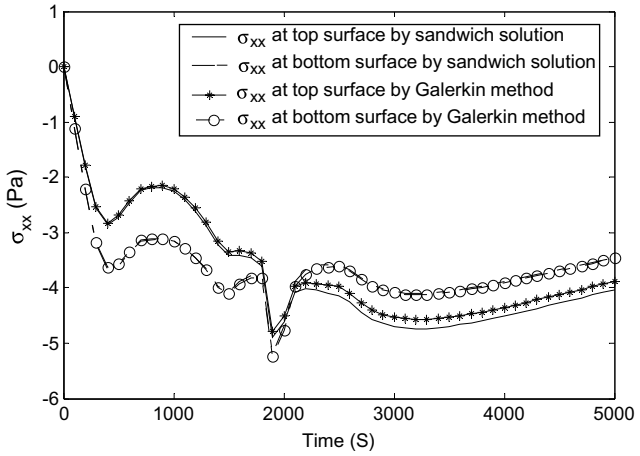

Fig. 6. History of normal stress (σ_{xx}) in structure of linear design ($L = 18$ in.).

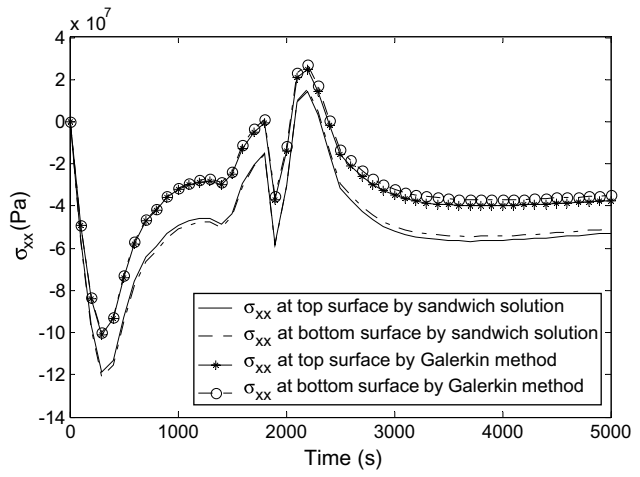

Fig. 7. History of normal stress (σ_{xx}) in top facesheet of linear design ($L = 9$ in.).

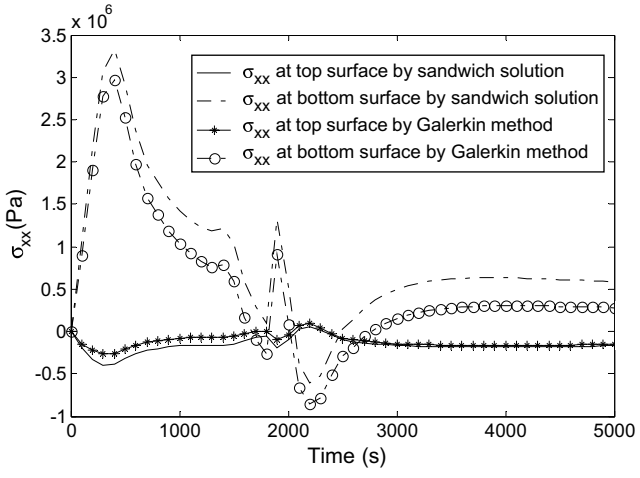

Fig. 8. History of normal stress (σ_{xx}) in top half core of linear design ($L = 9$ in.).

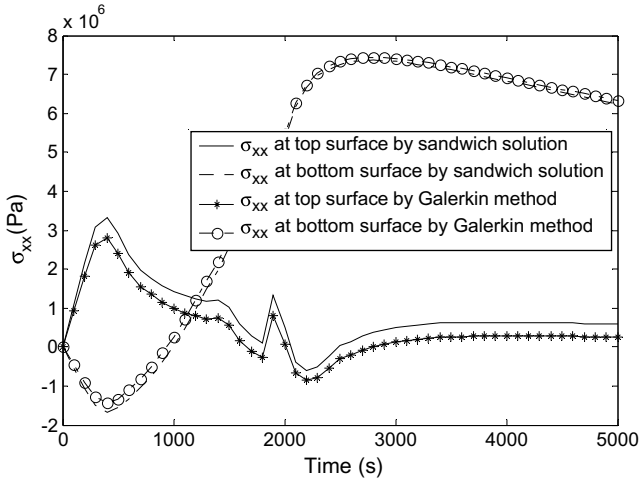

Fig. 9. History of normal stress (σ_{xx}) in bottom half core of linear design ($L = 9$ in.).

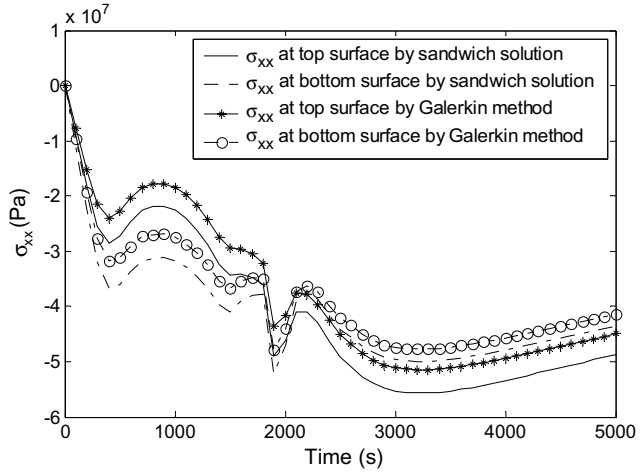

Fig. 10. History of normal stress (σ_{xx}) in structure of linear design ($L = 9$ in.).

insulation. For the purpose of comparison, the problem of a uniform foam design with same foam insulation weight, same top facesheet and structure is also solved. Figs. 11 and 12 show the temperature histories at top facesheet and structure, respectively. It is shown in Fig. 12 that maximum structural temperature can be reduced by 30 K by linearly varying the insulation foam solidity. This is achieved by increasing the top facesheet temperature faster to radiate out more heat for linear design compared with uniform design, as shown in Fig. 11. The histories of stress ratio, which is defined as the ratio between the stresses in each layer and temperature-dependent yield stress, are also plotted for each layer in Figs. 13–16. These four plots indicate that the maximum stress ratio in the base structure and foam core can be reduced 25% or more by linearly varying

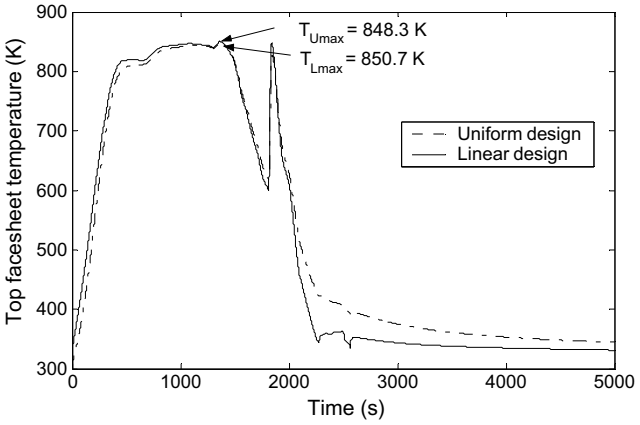

Fig. 11. Temperature history at top facesheet for both linear and uniform designs.

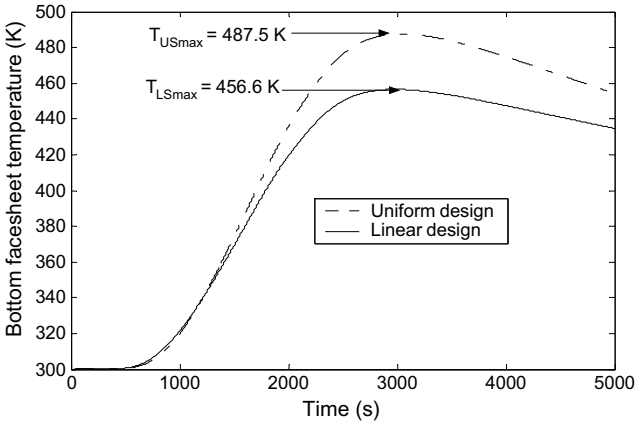

Fig. 12. Structural temperature history for both linear and uniform designs.

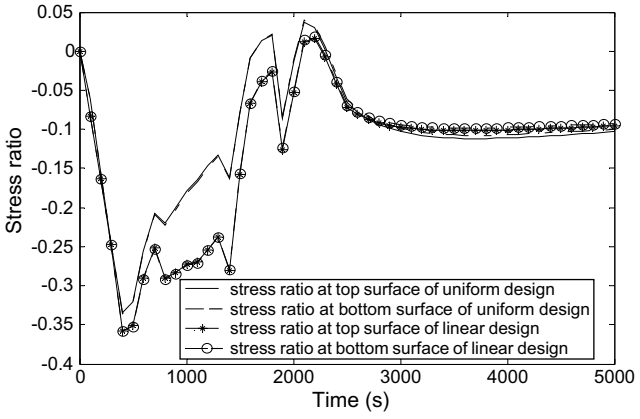

Fig. 13. History of normal stress (σ_{xx}) in top face sheet of uniform and linear design ($L = 18$ in.).

the foam solidity with only 5% increase in stress ratio in the top face sheet.

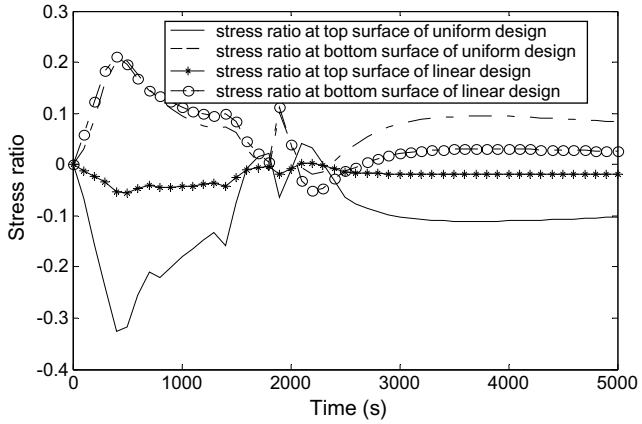

Fig. 14. History of normal stress (σ_{xx}) in top half core of uniform and linear design ($L = 18$ in.).

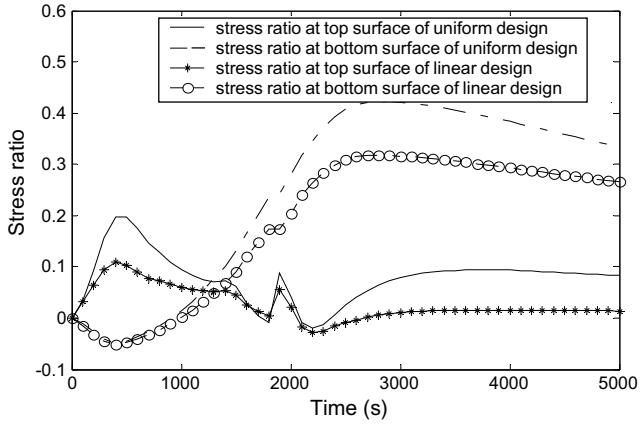

Fig. 15. History of normal stress (σ_{xx}) in bottom half core of uniform and linear design ($L = 18$ in.).

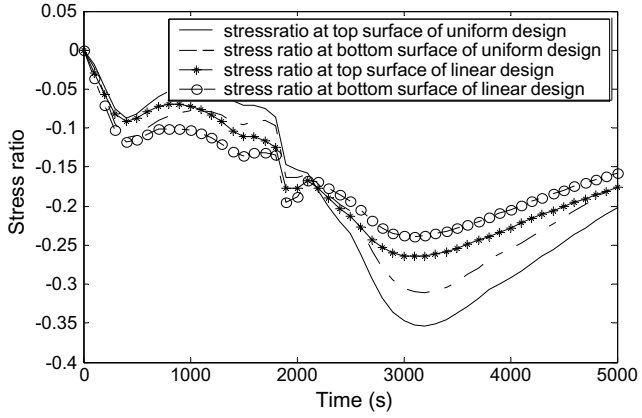

Fig. 16. History of normal stress (σ_{xx}) in structure of uniform and linear design ($L = 18$ in.).

5. Conclusions and future work

The analysis procedures developed in this paper will be useful in the optimization of the multilayer TPS structure subjected to temperature and stress constraints. The results suggest that classical lamination theory may not be suitable for the analysis of thick sandwich TPS panel and more accurate plate theories, e.g., higher order theories or new sandwich plate theories, need to be developed. One of the major issues in the TPS for RLVs is that the temperature attains the maximum after the vehicle has landed when the mechanical loads are minimum or almost do not exist. On the other hand during the beginning phase of the reentry the mechanical loads are high but the thermal loads are low. This situation offers an opportunity to optimize the TPS and minimize the mass. This problem will be considered in the future after developing more accurate sandwich plate theories for this purpose.

Acknowledgements

This research is supported by the NASA CUIP (formerly URETI) Grant NCC3-994 to the Institute for Future Space Transport (IFST) at the University of Florida. The cognizant program manager is Claudia Mayer at NASA Glenn Research Center.

References

[1] Blosser ML. Investigation of fundamental modeling and thermal protection issues for a metallic thermal protection system design. In: Proceedings of the 40th aerospace sciences meeting and exhibit, Reno, Nevada, 2002. AIAA paper 2002-0503.
[2] Blosser ML, Chen RR, Schmidt IH, Dorsey JT, Poteet CC, Bird RK. Advanced metallic thermal protections system development. In: Proceedings of the 40th aerospace sciences meeting and exhibit, Reno, Nevada, 2002. AIAA paper 2002-0504.
[3] Venkataraman S, Haftka RT, Sankar BV, Zhu H, Blosser ML. Optimal functionally graded metallic foam thermal insulation. AIAA J 2004;42(11):2355–63.
[4] Zhu H, Sankar BV, Haftka RT, Venkataraman S. Minimum mass design of insulation made of functionally graded material. In: Proceedings of the 43rd AIAA structures, structural dynamics and materials conference, Denver, Colorado, 2002. AIAA paper 2002-1425.
[5] Zhu H, Sankar BV, Haftka RT, Venkataraman, S. Optimization of a functionally graded metallic foam insulation under transient heat transfer conditions. In: Proceedings of the 44th AIAA structures, structural dynamics and materials conference, Norfolk, Virginia, 2003. AIAA paper 2003-1531.
[6] Sankar BV. An elasticity solution for functionally graded beams. Compos Sci Technol 2001;61:689–96.
[7] Sankar BV, Tzeng JT. Thermal stresses in functionally graded beams. AIAA J 2002;40(6):1228–32.
[8] Zhu H, Sankar BV, Haftka RT. Analysis of TPS sandwich panel with foam core. In: Proceedings of 45th AIAA structures, structural dynamics and materials conference, Palm Spring, California, 2004. AIAA paper 2004-1935.
[9] Choi S, Sankar BV. A micromechanical method to predict the fracture toughness of cellular materials. Int J Solids Struct 2005;42(2005):1797–817.